Hierarchical Ionic Self-Assembly of Rod−Comb Block Copolypeptide−Surfactant Complexes

Sirkku Hanski,[†] Nikolay Houbenov,[†] Janne Ruokolainen,[†] Dimitra Chondronicola,[‡] Hermis Iatrou,[‡] Nikos Hadjichristidis,*[,‡] and Olli Ikkala*[,†]

Department of Engineering Physics and Mathematics and Center for New Materials, Helsinki University of Technology, P.O. Box 2200, FIN-02015 HUT, Espoo, Finland and Chemistry Department, University of Athens, Panepistimiopolis, Zografou 15771, Athens, Greece

Received July 13, 2006; Revised Manuscript Received September 19, 2006

Novel hierarchical nanostructures based on ionically self-assembled complexes of diblock copolypeptides and surfactants are presented. Rod−coil diblock copolypeptide poly(γ-benzyl-L-glutamate)-*block*-poly(L-lysine), PBLG-*b*-PLL (M_n = 25 000 and 8000 for PBLG and PLL, respectively, polydispersity index 1.08), was complexed with anionic surfactants dodecanesulfonic acid (DSA) or dodecyl benzenesulfonic acid (DBSA), denoted as PBLG-*b*-PLL(DSA)$_{1.0}$ and PBLG-*b*-PLL(DBSA)$_{1.0}$, respectively. The complexation leading to supramolecular rod−comb architectures was studied by transmission electron microscopy (TEM), small-angle X-ray scattering (SAXS), Fourier transform infrared spectroscopy (FTIR), and polarized optical microscopy (POM). PBLG-*b*-PLL, PBLG-*b*-PLL(DBSA)$_{1.0}$, and PBLG-*b*-PLL(DSA)$_{1.0}$ self-assemble with alternating PBLG lamellae and PLL-containing lamellae with a periodicity of 27−33 nm. Within the PBLG lamellae, the rod-like PBLG helices pack with a periodicity of ca. 1.3 nm. The internal structure of the PLL-containing lamellae depends on the complexation. For pure PBLG-*b*-PLL, the PLL chains adopt a random coil conformation and the PLL domains are disordered. For PBLG-*b*-PLL(DSA)$_{1.0}$, lamellar self-assembly of periodicity of 3.7 nm within the PLL(DSA)$_{1.0}$ domains is observed due to crystalline packing of the linear *n*-dodecyl tails. For PBLG-*b*-PLL(DBSA)$_{1.0}$ with branched dodecyl tails, a distinct SAXS reflection is observed, suggesting self-assembly within the PLL(DBSA)$_{1.0}$ domains with a periodicity of 2.9 nm. However, due to the absence of higher order reflections, the internal structure cannot be conclusively assigned. The efficient plasticization which leads to fluid-like liquid crystallinity in PBLG-*b*-PLL-(DBSA)$_{1.0}$ and an α-helical conformation according to FTIR allows us to suggest that the PLL(DBSA)$_{1.0}$ domains have a hexagonal internal structure. The interplay of self-assembly at different length scales combined with rod-like liquid crystallinity can open new routes to design functional materials.

Introduction

Self-assembly leads to controlled nanoscale structures due to competing attractive and repulsive interactions.[1−5] Upon using constructional units of different natures and sizes one can efficiently tune the self-assembly into hierarchical organization. A repulsive interaction can be achieved based on immiscibility of different structural blocks in the solid or "melt" state. The undesirable macroscopic phase segregation between such blocks is prevented by attractive interactions due to covalent bonding, as in block copolymers,[1,2,6,7] or by sufficiently strong physical interactions.[5,8] A specific case of self-assembling materials is given by polymeric comb-shaped supramolecules consisting of repulsive flexible or mesogenic side chains which are bonded to the main chain ionically,[9−16] hydrogen bonding,[17−19] or coordination.[20,21] When block copolymers are incorporated, for example, with physically bonding surfactants or oligomeric amphiphiles to one of the blocks, complicated hierarchical structures are formed showing order at several length scales.[22−25] It is expected that an even higher level of structural controllability could be achieved when using polypeptides as constituent blocks since the polypeptides can fold to secondary structures like α helices and β sheets.

Synthetic polypeptides have been intensively studied, especially after the development of synthetic routes that allow narrow polydispersities.[26−29] Structures at several length scales and feasible properties have been observed for diblock copolymers in the solid state, where one of the blocks is a rod-like polypeptide and the other one is a flexible synthetic polymer.[30−33] For example, the self-assembly of oligo(γ-benzyl-L-glutamate)-*b*-oligo(styrene) can be controlled based on the block sizes.[30] On the other hand, the secondary structure and packing of the peptidic block in rod−coil poly(γ-benzyl-L-glutamate)-*b*-polystyrene and poly(*Z*-L-lysine)-*b*-polystyrene block copolymers contribute to the formation of novel phases.[31−33] More recently, substantial interest has been devoted to pure diblock copolypeptides.[34,35] Different rod- or coil-like polypeptides influence the phase behavior and cholesteric order in rigid-rod poly(γ-benzyl-L-glutamate)-based block copolypeptides.[34] Hierarchical cylindrical-*on*-hexagonal and cylindrical-*in*-lamellar morphologies have been shown based on block copolypeptides consisting of α-helical poly(γ-benzyl-L-glutamate) and poly(L-glycine) where the latter forms β sheets.[35]

Importantly, in addition to the structures in the solid state, the polypeptide-containing block copolymers have feasible properties in solution, including magnetic field controllable liquid crystallinity[36] or vesicle formation,[37] which can be stimuli responsive.[38,39] A number of studies have demonstrated that modification of polypeptides by covalently bound low molecular weight species can induce significant changes in their behavior

* To whom correspondence should be addressed. Olli.Ikkala@hut.fi, hadjichristidis@chem.uoa.gr.
[†] Helsinki University of Technology.
[‡] University of Athens.

10.1021/bm0606770 CCC: $33.50
Published on Web 11/15/2006

Table 1. Characteristics of the PBLG-*b*-PBocLL Block Copolypeptide

sample	M_n (kD)[a]	polydispersity index (SEC)	N_{PBLG}[b]	N_{PBocLL}[b]	%PBocLL (w/w)[c]
$PBLG_{123}$	27.1 (25.0)	1.09	123		
$PBLG_{123}$-*b*-$BocLL_{62}$	40.7 (38.2)	1.08	123	62	33.5 (34.6)

[a] By SEC-TALLS, in DMF/LiBr (0.1 N), at 60 °C. The calculated values from stoichiometry are given in parentheses. [b] Number of monomeric units. [c] By ^{1}H NMR in DMSO-d_6. The calculated values from the M_n value are given in parentheses.

and properties like melting temperature or degree of ordering in a liquid crystalline state.[40] On the other hand, complexation of ionic surfactants to homopolypeptides to form polyelectrolyte/surfactant complexes allows self-assembly and can induce conformational changes.[41−44]

In the present paper, we investigate the self-assembly of poly(γ-benzyl-L-glutamate)-*b*-poly(L-lysine) (PBLG-*b*-PLL) diblock copolypeptide upon ionic complexation of anionic surfactants dodecyl benzenesulfonic acid (DBSA) or dodecanesulfonic acid (DSA) to the cationic PLL block. Complexation between the anionic surfactants and the polycation chains occurs via proton transfer from the acid group to the base, resulting in electrostatically bonded comb-like structures. Ionic self-assembly due to surfactant binding has, to the best of our knowledge, not been investigated so far in the case of block copolypeptides in the solid state. We expected that the PBLG-*b*-PLL/surfactant system could allow interesting interplay of different ordering mechanisms, each at different length scales: the block copolymeric self-assembly, polyelectrolyte/surfactant self-assembly, and liquid crystallinity of the rod-like helices of PBLG[34,45] in combination with control of PLL secondary structures. The structures are studied using TEM, SAXS, FTIR, and POM.

Experimental

Synthesis of Poly(γ-benzyl-L-glutamate)-*b*-poly(ε-*tert*-butyloxycarbonyl-L-lysine). The synthesis of diprotected diblock copolypeptide poly(γ-benzyl-L-glutamate)-*b*-poly(ε-*tert*-butyloxycarbonyl-L-lysine) (PBLG-*b*-PBocLL) was performed by sequential ring-opening polymerization (ROP) of the corresponding *N*-carboxyanhydrides of γ-benzyl-L-glutamate (NCA-BLG) and ε-*tert*-butyloxycarbonyl-L-lysine (NCA-BocLL) in DMF with *n*-hexylamine as initiator using high-vacuum techniques (HVT).[46] HVT have been proven[29] to lead to living polypeptides in ∼100% yield, a necessary condition for the synthesis of well-defined block copolypeptides. The polymerization reactor, equipped with break seals to add reagents and constrictions to remove intermediate products, was appropriately designed in order to have at least three times larger volume than that of the CO_2 generated by each ROP. The combination of HVT and appropriate reactor volume forces polymerization to completion.

For the synthesis of the copolypeptide, the initiator solution (0.104 mmol in DMF, 1% w/w) and the first monomer NCA-BLG (2.6 g in DMF, 10% w/w) were introduced to the reactor and left to react. After ∼48 h a small aliquot was removed for characterization by heat sealing of a side tube. The second monomer (NCA-BocLL) was subsequently added (1.37 g, 10% w/w) and left to react for 4 days. The resulting block copolypeptide PBLG-*b*-PBocLL was precipitated in diethyl ether and dried under vacuum until constant weight. Both ROPs were monitored by size-exclusion chromatography (SEC). The number-average molecular weight M_n and the polydispersity index M_w/M_n of the PBLG block and the final PBLG-*b*-PBocLL are shown in Table 1 and were characterized by a SEC-UV instrument which featured a two-angle laser light scattering (SEC-TALLS) detector at 333 K and using a 0.1 N LiBr solution of DMF as the mobile phase. The low polydispersity indices along with the very good agreement between the stoichiometric and determined molecular weights reveal a high degree of molecular weight and compositional homogeneity. The composition of the copolypeptide PBLG-*b*-PBocLL, determined by ^{1}H NMR spectroscopy in $CDCl_3$, is in good agreement with the theoretical one calculated from M_n (data not shown).

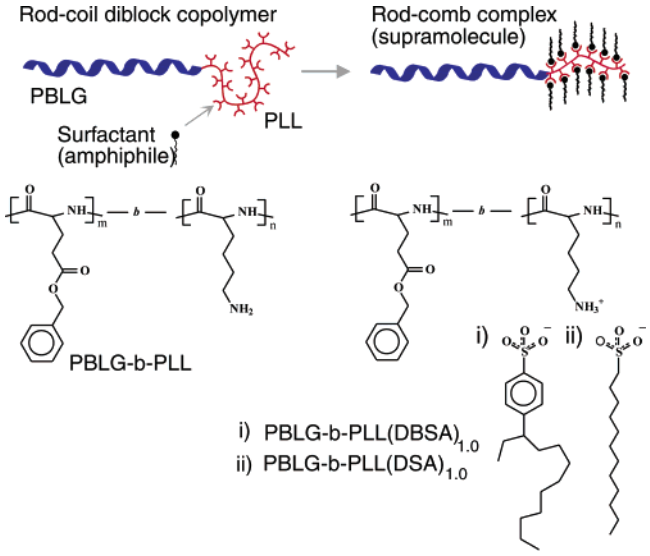

Figure 1. Schematic view of the diblock copolypeptide−surfactant complexes studied in this work. DBSA is shown in one of its possible branched alkyl tail structures.

Synthesis of Poly(γ-benzyl-L-glutamate)-*block*-poly(L-lysine). Selective deprotection of the ε-amine group of the BocLL block was achieved by dissolving the copolypeptides in trifluoroacetic acid (TFA) and allowing a reaction time of 2 h, followed by removal of the TFA by distillation on the vacuum line and elimination of the resulting salts by dialysis in a Milli-Q water-HCl mixture with pH 4.[47] The procedure was repeated 5 times. An additional dialysis was performed at pH 10.5. The ε-amine of the polylysine−HCl was thus transformed to the free amine group, as confirmed by NMR spectroscopy in DMSO-d_6 (data not shown). The deprotection resulted in PBLG-*b*-PLL with block sizes of M_n = 25 000 and 8000 g/mol, respectively.

Complex Preparation. Dodecyl benzenesulfonic acid soft type (DBSA) was purchased from Tokyo Kasei and *n*-dodecanesulfonic acid sodium salt from Sigma Aldrich. The sodium salt of dodecanesulfonic acid was transferred to an acid form (DSA) with ion-exchange resin Amberlite IR-120+ (Merck). Both surfactants have a dodecyl alkyl tail, but importantly, DBSA contains predominantly methyl or ethyl branching (see Figure 1) whereas DSA contains a linear unbranched alkyl tail. Such a slight irregularity of DBSA suppresses its crystalline packing. Trifluoroacetic acid (TFA) and chloroform (Aldrich) were used as received. The complexes were prepared from 12% v/w TFA/chloroform solvent mixtures with concentration of 0.5% w/w by slowly evaporating the solvent. A 1:1 molar ratio between the surfactant and a PLL repeat unit was used. The materials were further dried in a vacuum oven at room temperature for at least 2 h before measurements. In Figure 1, a schematic illustration of the block copolypeptide and the molecular formulas of the complexes are presented with the denotation of the complexes based on their nominal compositions PBLG-*b*-PLL$(DBSA)_{1.0}$ and PBLG-*b*-PLL$(DSA)_{1.0}$.

Transmission Electron Microscopy (TEM). A transmission electron microscope, FEI Tecnai 12, operating at 120 kV accelerating voltage was used for the morphological studies. Samples were cryomicrotomed with a Leica Ultracut UCT-ultramicrotome at −100 °C to 70 nm thick sections. The sections were stained at room temperature with osmium tetroxide (PBLG-*b*-PLL, 2 h) or ruthenium tetroxide (PBLG-*b*-PLL$(DSA)_{1.0}$ and PBLG-*b*-PLL$(DBSA)_{1.0}$, 30 min) to improve the contrast between the domains.

Small-Angle X-ray Scattering (SAXS). The periodicities of the structures were measured by small-angle X-ray scattering using a Bruker

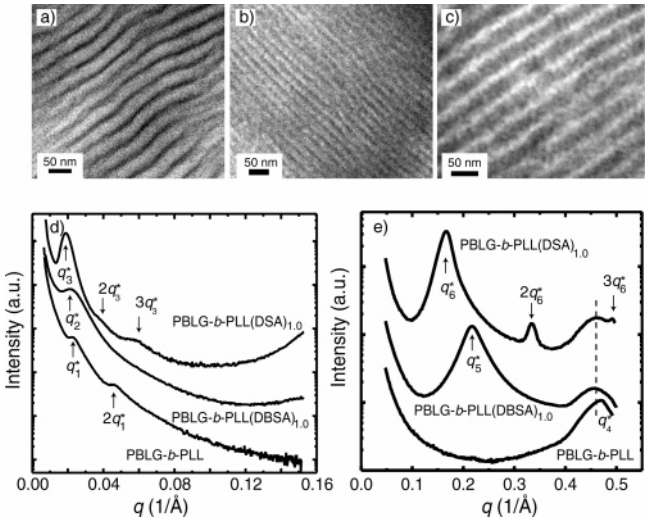

Figure 2. (Top) TEM micrographs of diblock copolypeptide−surfactant complexes for (a) PBLG-*b*-PLL, (b) PBLG-*b*-PLL(DBSA)$_{1.0}$, and (c) PBLG-*b*-PLL(DSA)$_{1.0}$. In (a) the PBLG block appears light and in (b) and (c) dark because of the different staining requirements. (Bottom) SAXS graphs showing the structures (d) at the diblock copolypeptide length scale and (e) at the surfactant length scale.

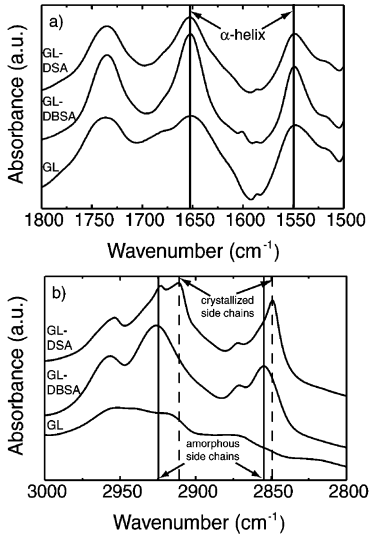

Figure 3. FTIR spectra of PBLG-*b*-PLL, PBLG-*b*-PLL(DBSA)$_{1.0}$, and PBLG-*b*-PLL(DSA)$_{1.0}$, denoted as GL, GL-DBSA, and GL-DSA, respectively. (a) Amide band range: the amide I at 1652 cm^{-1} and the amide II at 1549 cm^{-1} bands characteristic for α helix. Note the increased bands at ca. 1680 and 1535 cm^{-1} for PBLG-*b*-PLL, indicating more random coil characteristics attributed to the PLL block. Relatively narrow α-helix peaks are shown for PBLG-*b*-PLL(DBSA)$_{1.0}$, suggesting that PLL also adopts the α-helical conformation. (b) C−H stretching range: amorphous branched dodecyl chains with absorptions at 2926 and 2856 cm^{-1} in PBLG-*b*-PLL(DBSA)$_{1.0}$ and crystallized *n*-dodecyl chains with 2915 and 2850 cm^{-1} for PBLG-*b*-PLL(DSA)$_{1.0}$.

Microstar microfocus X-ray source with a rotating anode (Cu Kα radiation, $\lambda = 1.54$ Å) and Montel Optics. The beam was further collimated with four sets of four-blade slits resulting in a beam of about 1 mm × 1 mm at the sample position. The distance between the sample and the 2D detector (Bruker AXS) was set to 1.5 or 0.45 m for the different structure length scales. The magnitude of the scattering vector is given by $q = (4\pi/\lambda)\sin\theta$, where 2θ is the scattering angle.

Infrared Spectroscopy. Infrared spectra were recorded by Nicolet 380 FTIR spectrometer. Sixty-four scans were taken and averaged with a resolution of 2 cm^{-1}. FTIR samples were prepared by mixing the solid samples with KBr in a mortar, followed by pressing the mixture to pellets. The samples were dried in a vacuum for several hours before experiments.

Polarized Optical Microscopy. The birefringence was observed using a Nikon Type 104 optical microscope with crossed polarizers. The microscope was equipped with a JVC 3-CCD Color Video camera. The solid samples were inserted between a glass slide and a cover glass and gently pressed.

Results and Discussion

The structural hierarchy at the diblock copolypeptide and the surfactant length scales, i.e., at tens of nanometers and a few nanometers length scales, were studied by TEM and SAXS and supported by FTIR and POM. Figure 2 shows the TEM micrographs of PBLG-*b*-PLL, PBLG-*b*-PLL(DBSA)$_{1.0}$, and PBLG-*b*-PLL(DSA)$_{1.0}$. In all cases, a well-defined lamellar structure is observed at the diblock copolypeptide length scale. We point out that due to the softness of the samples, compression took place during the ultramicrotoming, and therefore, a quantitative determination of periodicities cannot be done based on TEM. Smaller surfactant-level structures were not resolved in TEM. However, the SAXS measurement showed reflections both at the diblock copolypeptide and surfactant length scales (see Figure 2d and e). PBLG-*b*-PLL has a reflection at $q_1^* = 0.023$ Å^{-1} corresponding to a periodicity of 27 nm and a second-order reflection at $2q_1^*$, suggesting lamellar order in agreement with TEM. PBLG-*b*-PLL(DBSA)$_{1.0}$ has only one broad reflection at $q_2^* = 0.022$ Å^{-1}, which corresponds to a periodicity of 29 nm, but can also be assigned as lamellar based on TEM. PBLG-*b*-PLL(DSA)$_{1.0}$ shows a clear main reflection at $q_3^* = 0.019$ Å^{-1}, a faint reflection at $2q_3^*$, and a more clear reflection at $3q_3^*$, indicating lamellar order with a periodicity of 33 nm. As expected, the periodicities of the lamellar structures at the polypeptide length scale increase upon adding the surfactants. However, even if DSA has a smaller molecular weight than DBSA, it causes a significantly larger periodicity at the block copolymer length scale, the reason of which will be discussed later. Figure 2e depicts SAXS at larger scattering angles in order to study the surfactant-level structures. A broad reflection at $q_4^* = 0.47$ Å^{-1} was observed for pure PBLG-*b*-PLL, corresponding to a periodicity of 1.3 nm, which can be assigned to the hexagonal packing of PBLG helices.[34,45] Such a helical packing of PBLG is observed also for PBLG-*b*-PLL(DBSA)$_{1.0}$, but in addition, there exists a strong reflection at $q_5^* = 0.22$ Å^{-1}, corresponding to a structure with a periodicity of ca. 2.9 nm. Higher order reflections are not resolved. For PBLG-*b*-PLL(DSA)$_{1.0}$ the PBLG helical packing is also observed. Furthermore, even more pronounced ordering takes place as SAXS shows reflections at $q_6^* = 0.17$ Å^{-1}, $2q_6^*$, and $3q_6^*$, indicating lamellar organization with a periodicity of 3.7 nm. Note that this is almost 1 nm larger than the periodicity in PBLG-*b*-PLL(DBSA)$_{1.0}$, suggesting that the surfactants can control the self-assembly in a delicate manner. In conclusion, structures with periodicities of ca. 30 and 3 as well as 1.3 nm are observed indicating a hierarchical self-assembly.

In order to resolve the structural hierarchy, FTIR provided information, on one hand, on the secondary structure of the polypeptides and, on the other hand, on the conformation of the alkyl tails and therefore on the packing of the surfactant molecules. First, the absorption bands in the 1500−1800 cm^{-1} range will be discussed (see Figure 3a) as they include the amide I (1680−1630 cm^{-1}) and amide II (1570−1515 cm^{-1}) bands that are characteristic of the polypeptide conformation. In all compounds PBLG-*b*-PLL, PBLG-*b*-PLL(DBSA)$_{1.0}$, and PBLG-*b*-PLL(DSA)$_{1.0}$ a distinct absorption was observed at 1652 and

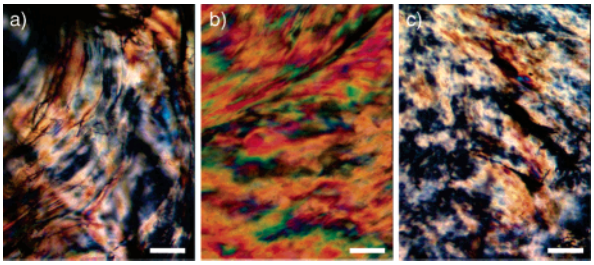

Figure 4. Polarized optical micrographs of the supramolecular complexes and pure polymer: (a) PBLG-*b*-PLL, (b) PBLG-*b*-PLL-$(DBSA)_{1.0}$, and (c) PBLG-*b*-PLL$(DSA)_{1.0}$. The scale bar is 50 μm.

1549 cm^{-1}, indicating that they all contain a major fraction of α helices. This is not surprising since, e.g., PBLG-*b*-PLL contains 76% w/w of PBLG, which tends to fold in a helical manner. Considering also the SAXS results (Figure 2d and 2e), we assign the PBLG chain to adopt α-helical conformation (see also a later discussion in the context of Figure 5). A closer look of Figure 3a shows that PBLG-*b*-PLL has significantly broadened amide I and amide II bands, and two faint shoulders can be resolved on both sides of the main amide I band. Such a broadening suggests that PBLG-*b*-PLL contains a mixture of other types of secondary structures in addition to the α helices. Therefore, we propose that PLL adopts a random coil conformation. Upon complexing with DBSA, the amide I and amide II peaks at 1652 and 1549 cm^{-1} become distinctly narrower. This suggests a well-defined α-helical conformation for the whole PBLG-*b*-PLL$(DBSA)_{1.0}$ backbone, even for the PLL block in addition to the PBLG block. This narrowing is less pronounced for PBLG-*b*-PLL$(DSA)_{1.0}$, implicating differences in the PLL conformation due to different surfactants. Figure 3b shows the 2800−3000 cm^{-1} bands, which are sensitive for alkyl chain conformations. The absorptions at 2915 and 2850 cm^{-1} reveal partial *n*-dodecyl side chain crystallization in PBLG-*b*-PLL$(DSA)_{1.0}$, whereas the alkyl chains of DBSA remain amorphous (2926 and 2856 cm^{-1}). The alkyl chain crystallization in PBLG-*b*-PLL$(DSA)_{1.0}$ in comparison with the amorphous side chains of PBLG-*b*-PLL$(DBSA)_{1.0}$ is suggested to have a pronounced effect on the self-assembled structures.

The effect of added surfactants manifests also in optical microscopy. Pure PBLG-*b*-PLL does not flow at room temperature upon pressing between two microscope slides. The material shows strong birefringence (Figure 4a), which is not surprising as the PBLG-*b*-PLL contains 76% w/w of helical rod-like PBLG chains. Previously it has been observed with other PBLG-containing block copolypeptides that rod-like PBLG leads to liquid crystallinity even if its weight fraction falls below 50% w/w.[34] PBLG-*b*-PLL$(DBSA)_{1.0}$ behaves dramatically differently. DBSA with its branched alkyl tails allows efficient plasticization, and therefore, the material flows upon pressing between two microscope glass plates. As birefringence in the fluid state is observed in POM, one can conclude that PBLG-*b*-PLL-$(DBSA)_{1.0}$ is liquid crystalline (Figure 4b). Note that previously studied DBSA complexation with basic polymers is known to allow efficient plasticization even for rigid conjugated polymers.[48−50] On the other hand, covalently bonded side chains in the polypeptides have also been found to allow plasticization of rod-like chains, which leads to liquid crystallinity.[51] Therefore, we suggest that in the present case the DBSA complexation leads to fluid-like plasticization of the PLL α helices. By contrast, in the PBLG-*b*-PLL$(DSA)_{1.0}$ complex partial crystallization of the straight *n*-dodecyl tails locks the structure leading to a hard material, and in POM the material shows birefringence rather with crystalline pattern (Figure 4c).

Summarizing the results from TEM, SAXS, FTIR, and POM, we suggest three different types of self-assembled structures, presented schematically in Figure 5. On the basis of TEM and SAXS, a lamellar order at the diblock copolypeptide length scale was observed for all materials. We will first give arguments for the hexagonal packing of rod-like PBLG helices in an interdigitated manner. The calculated length of a helical PBLG rod is ca. 18 nm based on the number of repeat units $m = 123$ (Table 1) and the pitch of the α helix $l = 1.5$ Å.[52] In the pure PBLG-*b*-PLL the periodicity was 27 nm based on SAXS ($q_1^* = 0.023$ $Å^{-1}$), which suggests extended rod-like PBLG helices instead of their folding. The thickness of the PLL lamellae is then ca. 9 nm, which indicates that the PLL chains adopt random coil conformation in order to fill the volume at the block interfaces. This resembles previously reported structures in different but related copolypeptides[53,54] with an antiparallel, i.e., interdigitating, orientation of the PBLG rods. This packing allows a favorable orientation of the dipole moments in the α helices[55] and minimization of the steric and/or interelectrostatic repulsion between the PLL chains at both peripheral ends. At the shorter scale, only one significant SAXS reflection in PBLG-*b*-PLL is observed at $q_4^* = 0.47$ $Å^{-1}$, which corresponds to the 1.3 nm periodicity between the hexagonally packed PBLG helices.[34,45] The PLL block does not show clear order in the block copolypeptide PBLG-*b*-PLL (Figure 3), even if homopolymeric PLL readily forms secondary structures (often β sheets). This can be explained by the small size of the PLL block (24% w/w) as compared to the PBLG block. The PBLG block dominates the self-assembly, while the PLL block adopts flexible random coil conformation and fills up the space at the end of the PBLG helices, as discussed above. Hence, one can conclude that pure PBLG-*b*-PLL shows well-defined lamellar order with alternating PBLG and PLL domains. The PBLG domains contain hexagonally packed extended PBLG helices, and the PLL domains are disordered due to coil-like PLL chains. The structure could be denoted as a hexagonal-*in*-lamellar structure (Figure 5a).

It is helpful next to discuss PBLG-*b*-PLL$(DSA)_{1.0}$ where the *n*-dodecyl tails of DSA allow a detailed assignment of the structural hierarchy (see Figure 5c). SAXS shows lamellar order with a periodicity of 33 nm (Figure 2d), lamellar order with a periodicity of 3.7 nm (Figure 2e), in addition to the observed packing of the PBLG helices with a periodicity 1.3 nm (Figure 2e). This implies alternating lamellae of PBLG and PLL$(DSA)_{1.0}$ where the complexation of DSA to PBLG-*b*-PLL leads to an increase in the periodicity from 27 to 33 nm, see Figure 6. Within the PBLG lamellae, the chains are packed as rod-like α helices in an antiparallel fashion. Within the PLL$(DSA)_{1.0}$ lamellae, there exists lamellar self-assembly at a periodicity of 3.7 nm with alternating PLL and DSA layers, where the alkyl chain ends are packed in the crystalline state. The different levels of order are strongly related. The increase in the block copolypeptide length scale is provided by the effect of the regular, crystallized alkyl chain ends in the surfactant, which limits the conformational freedom of the PLL chains in comparison to the disordered PLL chains of PBLG-*b*-PLL. Previous studies of homopolymeric PLL$(DSA)_{1.0}$ cast from aqueous solutions[56] showed a lamellar organization of β-sheet structures with a periodicity of ca. 4 nm, and no crystallization of the alkyl chains was observed. Only after increasing the alkyl chain length to 16 methyl units (homopolymeric PLL/cetyl sulfonate), crystallization took place with interdigitated cetyl chains. However, in the present diblock copolypeptide complex PBLG-*b*-PLL$(DSA)_{1.0}$, crystallization of the surfactant chains

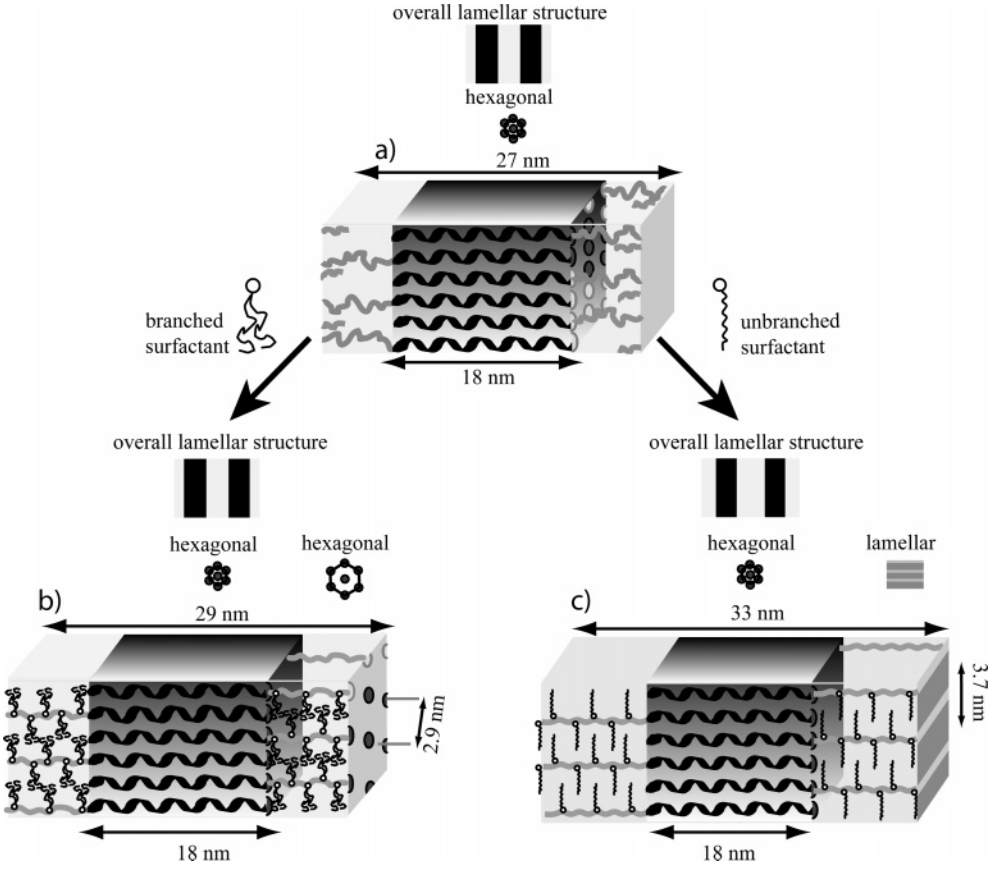

Figure 5. Proposed structures (strongly idealized). In all cases a lamellar overall order with alternating PBLG layers and PLL-containing layers is observed. The overall periodicity depends on the surfactant−PLL complexes. The PBLG chains are packed as rod-like helices within the PBLG domains. (a) In PBLG-*b*-PLL, the PLL domains have disordered internal structure. (b) In PBLG-*b*-PLL(DBSA)$_{1.0}$, FTIR suggests an α-helical conformation of PLL, and plasticization to fluid-like liquid crystal suggests a hexagonal assembly for PLL(DBSA)$_{1.0}$. We point out that the assignment of the PLL(DBSA)$_{1.0}$ internal structure remains tentative. (c) In PBLG-*b*-PLL(DSA)$_{1.0}$, there exists another lamellar self-assembly within PLL-(DSA)$_{1.0}$ due to alternating PLL and DSA layers. Here the crystalline packing of *n*-dodecyl tails plays a role.

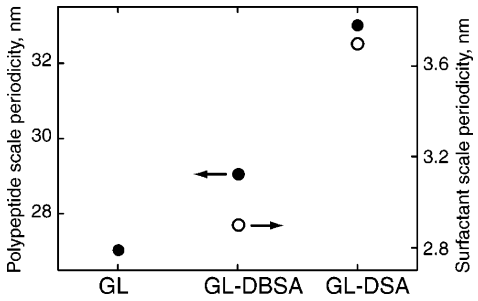

Figure 6. Influence of different surfactants to the self-assembled periodicities of the PBLG-*b*-PLL, PBLG-*b*-PLL(DBSA)$_{1.0}$, and PBLG-*b*-PLL(DSA)$_{1.0}$ denoted in the figure as GL, GL-DBSA, and GL-DSA, respectively.

was observed even for the *n*-dodecyl tails of DSA (FTIR in Figure 3b), probably because of the constraints set by the PBLG blocks. A simple geometrical reasoning suggests C_{12} interdigitations enabling crystallization and reducing the distance from maximum achievable 4.4 to 3.7 nm. In conclusion, PBLG-*b*-PLL(DSA)$_{1.0}$ shows alternating lamellae of PBLG and PLL-(DSA)$_{1.0}$, hexagonal packing of PBLG rod-like helices, and lamellar order of alternating PLL and DSA, i.e., hexagonal-*and*-lamellar-*in*-lamellar hierarchical structure (Figure 5c).

Finally, upon complexing DBSA to the PBLG-*b*-PLL, the periodicity at the polypeptide length scale increases from 27 to 29 nm ($q_2^* = 0.022$ Å^{-1}), see Figure 6. Although the block copolypeptide level order seems to be reduced upon complexation, a pronounced SAXS reflection at $q_5^* = 0.22$ Å^{-1} corresponding to ca. 2.9 nm emerges due to self-assembly within PLL(DBSA)$_{1.0}$ (Figure 2e). Referring to the FTIR results in Figure 3a, we suggest that the PLL chains in PBLG-*b*-PLL-(DBSA)$_{1.0}$ adopt an α-helical secondary structure. These results are in good agreement with our more comprehensive studies on homopolymeric PLL/DBSA complexes prepared from TFA/$CHCl_3$ solution showing hexagonally packed α helices[57] and previous work on the secondary structure of polylysine−surfactant complexes by others.[58,59] Even if the SAXS reflection at $q_5^* = 0.22$ Å^{-1} is distinct, higher order reflections cannot be resolved, and thus, the internal self-assembled structure within the PLL(DBSA)$_{1.0}$ domains remains unresolved conclusively. Two structures could be proposed: either the PLL α helices pack hexagonally with radial arrangement of DBSA molecules around the helices or the PLL α helices and DBSA form alternating lamellar layers. We expect that the latter structure would be less plasticized due to lamellar packing of rods within the lamellae. We would also foresee a tendency to transform the PLL α helices to β sheets if the PLL chains were closely packed within layers, which would not correlate with the FTIR data (Figure 3a). As we observed efficient plasticization of PBLG-*b*-PLL(DBSA)$_{1.0}$ to fluid-like liquid crystallinity even at room temperature, we are tempted to prefer the first structure. In this case the structure would consist of alternating PBLG and PLL(DBSA)$_{1.0}$ layers, where PBLG domains contain hexagonally packed rod-like α helices and the PLL(DBSA)$_{1.0}$ layers contain hexagonally packed PLL α helices separated by radial DBSA molecules. This could be denoted as hierarchical hexagonal-*and*-hexagonal-*in*-lamellar rod−comb structure (Figure 5b).

We finally point out that in PBLG-*b*-PLL(DBSA)$_{1.0}$ and PBLG-*b*-PLL(DSA)$_{1.0}$ there might exist a relatively thick disordered interfacial layer between the PBLG and PLL/surfactant domains to allow adaptation between the different structures and periodicities. In addition, minor structural differences were observed between parallel samples reflecting some process dependence. This is not surprising as high-temperature annealing cannot easily be done due to the possibility for irreversible conformational transitions of the polypeptides

Conclusions

We demonstrated that ionic complexation of surfactants DSA (linear *n*-dodecyl tail) and DBSA (branched dodecyl tail) to the coil-like PLL block of the rod−coil PBLG-*b*-PLL diblock copolypeptide leads to ionically self-assembled rod−comb complexes. This offers new possibilities to manipulate and tune polypeptide secondary structures in constructing complicated hierarchical nanostructures through self-assembly. The structural hierarchy was achieved by an interplay between diblock copolypeptide self-assembly at the tens of nanometers length scale, polyelectrolyte/surfactant self-assembly, which controls the PLL secondary structure at an order of magnitude smaller length scale, and packing of rod-like PBLG helices with 1.3 nm periodicity. Such concepts could pave the way for tailoring new materials for the interface between biological and functional synthetic matter and their compatibility.

Acknowledgment. We are grateful to Panu Hiekkataipale for his assistance in the SAXS measurements. We acknowledge funding from the Marie Curie Network BioPolySurf, Finnish National Agency for Technology and Innovation (project SMASM), and Academy of Finland (O.I. and J.R.). This work was carried out in the Centre of Excellence of Academy of Finland ("Bio- and Nanopolymers Research Group", 77317).

References and Notes

(1) Bates, F. S.; Fredrickson, G. H. *Phys. Today* **1999**, *52*, 32−38.
(2) Muthukumar, M.; Ober, C. K.; Thomas, E. L. *Science* **1997**, *277*, 1225−1232.
(3) Whitesides, G. M.; Mathias, J. P.; Seto, C. T. *Science* **1991**, *254*, 1312−1319.
(4) Whitesides, G. M.; Grzybowski, B. *Science* **2002**, *295*, 2418−2421.
(5) Ikkala, O.; ten Brinke, G. *Science* **2002**, *295*, 2407−2409.
(6) Bates, F. S.; Fredrickson, G. H. *Annu. Rev. Phys. Chem.* **1990**, *41*, 525−557.
(7) Hamley, I. W. *The Physics of Block Copolymers*; Oxford University Press: Oxford, 1998.
(8) Brunsveld, L.; Folmer, B. J. B.; Meijer, E. W.; Sijbesma, R. P. *Chem. Rev.* **2001**, *101*, 4071−4097.
(9) Antonietti, M.; Conrad, J.; Thünemann, A. *Macromolecules* **1994**, *27*, 6007−6011.
(10) Antonietti, M.; Förster, S.; Zisenis, M.; Conrad, J. *Macromolecules* **1995**, *28*, 2270−2275.
(11) Chen, H.-L.; Hsiao, M.-S. *Macromolecules* **1999**, *32*, 2967−2973.
(12) Faul, C. F. J.; Antonietti, M. *Adv. Mater.* **2003**, *15*, 673−683.
(13) Ikkala, O.; Ruokolainen, J.; ten Brinke, G.; Torkkeli, M.; Serimaa, R. *Macromolecules* **1995**, *28*, 7088−7094.
(14) Ober, K.; Wegner, G. *Adv. Mater.* **1997**, *9*, 17−31.
(15) Thünemann, A. F. *Prog. Polym. Sci.* **2002**, *27*, 1473−1572.
(16) Bazuin, C. G.; Brandys, F. A. *Chem. Mater.* **1992**, *4*, 970−972.
(17) Kato, T.; Fréchet, J. M. J. *Macromolecules* **1989**, *22*, 3818−3819.
(18) Ruokolainen, J.; Tanner, J.; Ikkala, O.; ten Brinke, G.; Thomas, E. L. *Macromolecules* **1998**, *31*, 3532−3536.
(19) Ruokolainen, J.; ten Brinke, G.; Ikkala, O.; Torkkeli, M.; Serimaa, R. *Macromolecules* **1996**, *29*, 3409−3415.
(20) Kurth, D. G.; Lehmann, P.; Schütte, M. *Proc. Natl. Acad. Sci. U.S.A.* **2000**, *97*, 5704−5707.
(21) Valkama, S.; Lehtonen, O.; Lappalainen, K.; Kosonen, H.; Castro, P.; Repo, T.; Torkkeli, M.; Serimaa, R.; ten Brinke, G.; Leskelä, M.; Ikkala, O. *Macromol. Rapid Commun.* **2003**, *24*, 556−560.
(22) Ruokolainen, J.; Saariaho, M.; Ikkala, O.; ten Brinke, G.; Thomas, E. L.; Torkkeli, M.; Serimaa, R. *Macromolecules* **1999**, *32*, 1152−1158.
(23) Ruokolainen, J.; ten Brinke, G.; Ikkala, O. *Adv. Mater.* **1999**, *11*, 777−780.
(24) Ikkala, O.; ten Brinke, G. *Chem. Commun.* **2004**, 2131−2137.
(25) Ruokolainen, J.; Mäkinen, R.; Torkkeli, M.; Mäkelä, T.; Serimaa, R.; Ten Brinke, G.; Ikkala, O. *Science* **1998**, *280*, 557−560.
(26) Deming, T. J. *Nature* **1997**, *390*, 386−389.
(27) Deming, T. J. *J. Polym. Sci., Part A: Polym. Chem.* **2000**, *38*, 3011−3018.
(28) Dimitrov, I.; Kukula, H.; Cölfen, H.; Schlaad, H. *Macromol. Symp.* **2004**, *215*, 383−393.
(29) Aliferis, T.; Iatrou, H.; Hadjichristidis, N. *Biomacromolecules* **2004**, *5*, 1653−1656.
(30) Klok, H.-A.; Langenwalter, J. F.; Lecommandoux, S. *Macromolecules* **2000**, *33*, 7819−7826.
(31) Losik, M.; Kubowicz, S.; Smarsly, B.; Schlaad, H. *Eur. Phys. J. E* **2004**, *15*, 407−411.
(32) Schlaad, H.; Kukula, H.; Smarsly, B.; Antonietti, M.; Pakula, T. *Polymer* **2002**, *43*, 5321−5328.
(33) Schlaad, H.; Smarsly, B.; Losik, M. *Macromolecules* **2004**, *37*, 2210−2214.
(34) Minich, E. A.; Nowak, A. P.; Deming, T. J.; Pochan, D. J. *Polymer* **2004**, *45*, 1951−1957.
(35) Papadopoulos, P.; Floudas, G.; Schnell, I.; Aliferis, T.; Iatrou, H.; Hadjichristidis, N. *Biomacromolecules* **2005**, *6*, 2352−2361.
(36) Bellomo, E. G.; Davidson, P.; Impéror-Clerc, M.; Deming, T. J. *J. Am. Chem. Soc.* **2004**, *126*, 9101−9105.
(37) Kukula, H.; Schlaad, H.; Antonietti, M.; Förster, S. *J. Am. Chem. Soc.* **2002**, *124*, 1658−1663.
(38) Bellomo, E. G.; Wyrsta, M. D.; Pakstis, L.; Pochan, D. J.; Deming, T. J. *Nat. Mater.* **2004**, *3*, 244−248.
(39) Chécot, F.; Lecommandoux, S.; Klok, H.-A.; Gnanou, Y. *Eur. Phys. J. E* **2003**, *10*, 25−35.
(40) Schaefer, K. E.; Keller, P.; Deming, T. J. *Macromolecules* **2006**, *39*, 19−22.
(41) Gallot, B. *Prog. Polym. Sci.* **1996**, *21*, 1035−1088.
(42) Liu, J.; Takisawa, N.; Kodama, H.; Shirahama, K. *Langmuir* **1998**, *14*, 4489−4494.
(43) MacKnight, W. J.; Ponomarenko, E. A.; Tirrell, D. A. *Acc. Chem. Res.* **1998**, *31*, 781−788.
(44) Roscigno, P.; D'Auria, G.; Falcigno, L.; D'Errico, G.; Paduano, L. *Langmuir* **2005**, *21*, 8123−8130.
(45) Floudas, G.; Papadopoulos, P.; Klok, H.-A.; Vandermeulen, G. W. M.; Rodriguez-Hernandez, J. *Macromolecules* **2003**, *36*, 3673−3683.
(46) Hadjichristidis, N.; Iatrou, H.; Pispas, S.; Pitsikalis, M. *J. Polym. Sci., Part A: Polym. Chem.* **2000**, *38*, 3211−3234.
(47) Greene, T. W.; Wuts, P.G. *Protective Groups in Organic Synthesis*; John Wiley & Sons, Inc.: New York, 1999.
(48) Cao, Y.; Smith, P.; Heeger, A. J. *Synth. Met.* **1992**, *48*, 91−97.
(49) Zheng, W.-Y.; Wang, R.-H.; Levon, K.; Rong, Z. Y.; Taka, T.; Pan, W. *Macromol. Chem. Phys.* **1995**, *196*, 2443−2462.
(50) Vikki, T.; Ruokolainen, J.; Ikkala, O. T.; Passiniemi, P.; Isotalo, H.; Torkkeli, M.; Serimaa, R. *Macromolecules* **1997**, *30*, 4064−4072.
(51) Watanabe, J.; Fukuda, Y.; Gehani, R.; Uematsu, I. *Macromolecules* **1984**, *17*, 1004−1009.
(52) Douy, A.; Gallot, B. *Polymer* **1982**, *23*, 1039−1044.
(53) Kim, K. T.; Park, C.; Vandermeulen, G. W. M.; Rider, D. A.; Kim, C.; Winnik, M. A.; Manners, I. *Angew. Chem., Int. Ed.* **2005**, *44*, 7964−7968.
(54) Kim, K. T.; Park, C.; Kim, C.; Winnik, M. A.; Manners, I. *Chem. Comm.* **2006**, 1372−1374.
(55) Yen, C.-C.; Tokita, M.; Park, B.; Takezoe, H.; Watanabe, J. *Macromolecules* **2006**, *39*, 1313−1315.
(56) Hanski, S.; Junnila, S.; Ikkala, O. Unpublished work.
(57) Hanski, S.; Junnila, S.; Ruokolainen, J.; Ikkala, O. Manuscript in preparation.
(58) Ponomarenko, E. A.; Tirrell, D. A.; MacKnight, W. J. *Macromolecules* **1996**, *29*, 8751−8758.
(59) Thünemann, A. F.; Beyermann, J.; Kukula, H. *Macromolecules* **2000**, *33*, 5906−5911.

BM0606770